ChemComm

Cite this: *Chem. Commun.*, 2011, **47**, 8100–8102

www.rsc.org/chemcomm

COMMUNICATION

Large-scaled star-shaped α-MnS nanocrystals with novel magnetic properties†

Qiwei Tian,[a] Minghua Tang,[a] Feiran Jiang,[a] Yiwei Liu,[b] Jianghong Wu,[a] Rujia Zou,[a] Yangang Sun,[a] Zhigang Chen,[a] Runwei Li[b] and Junqing Hu*[a]

Received 21st March 2011, Accepted 26th May 2011
DOI: 10.1039/c1cc11621e

A cooperative thermal decomposition route to large-scaled star-shaped α-MnS nanocrystals, which show novel magnetic properties, *i.e.*, a high blocking temperature (275 K) and a large coercive field (1573 Oe), is reported.

Significant efforts have been made to control the size and shape of inorganic nanocrystals (NCs), since these parameters strongly influence their physical properties.[1,2] New functional materials and further applications might emerge if inorganic NCs can be synthesized with complex shapes and well-defined three-dimensional (3D) architectures.[3–6] Usually, shape and morphology control are reliant on anisotropic nanocrystal nucleation and growth using a liquid medium, involving the use of a static template and surfactant.[7–10] Manganese sulfide (MnS), a magnetic semiconductor with a wide gap (E_g ~3.7 eV), can crystallize into three kinds of structural forms: the rock salt α-MnS, the zinc-blends β-MnS, and the wurtzite γ-MnS; it has potential applications in solar cells as a window/buffer material, dilute magnetic material,[11] in short wavelength optoelectronic devices[12] and Li-batteries.[13] So far, a considerable effort has been devoted to synthesize MnS NCs with a few shapes including spheres, cubes, pyramids, hexagonal rings,[14–21] and so on. However, these reported MnS NCs have not been demonstrated to possess interesting physical properties, which are imperative for the success of bottom-up nanodevice applications. Therefore, the development of not only facile but also architectural control of MnS anisotropic 3D NCs having novel physical properties is of significance. Herein, we report a simple controllable thermal decomposition route to large-scaled star-shaped α-MnS 3D NCs; these MnS NCs show novel magnetic properties, *i.e.*, a high blocking temperature (275 K) and a large coercive field (1573 Oe).

[a] *State Key Laboratory for Modification of Chemical Fibers and Polymer Materials, College of Materials Science and Engineering, Donghua University, Shanghai 201620, China. E-mail: hu.junqing@dhu.edu.cn; Fax: 86-21-6779-2947; Tel: 86-21-6779-2947*
[b] *Key Laboratory of Magnetic Materials and Devices, Ningbo Institute of Material Technology and Engineering (NIMTE), Chinese Academy of Sciences (CAS), Ningbo, Zhejiang 315201, China*

† Electronic supplementary information (ESI) available: Detailed experimental procedures; TEM images of the morphology evolution under different conditions. See DOI: 10.1039/c1cc11621e

In a typical thermal decomposition process, Mn oleate and sulfur with a mole ratio of 1 : 2 were used as source materials, and 1-octadecene (ODE) and a mixture of oleic acid (OA), oleyl amine (OM) and ODE with a volume ratio of 18 : 1 : 1 serve as a reaction solutions, respectively, and thermal decompositions were carried out at 280 °C and under N_2 atmosphere, as schematically shown in Fig. 1a. As shown from transmission electron microscope (TEM; JEM-2010F) images in Fig. 1b–e, the above two different reaction solutions resulted in the formation of two different shaped NCs. Using ODE as the reaction solution, the resulted product displays spherical monodispersed particles with a diameter of ~15 nm, Fig. 1b. A typical high-resolution TEM (HRTEM) image of a NC exhibits clear (200) (~0.261 nm) lattice fringes of cubic α-MnS crystal, confirming its high crystallinity, Fig. 1c. Using a mixture of OA, OM and ODE as a reaction solution, the resultant product shows a different morphology from the former, *i.e.*, star-shaped monodispersed particles with a mean diameter of 45 nm, Fig. 1d. A HRTEM image of this star-shaped NC also reveals (200) lattice fringes of crystalline α-MnS, Fig. 1e. These results suggest that we can readily control the morphologies of the α-MnS NCs by simply adjusting the volumes of the OA and OM in the ODE solution, while other parameters are kept constant.

An X-ray power diffraction (XRD; D/max-2550 PC) pattern in Fig. 2 displays the overall phase structure and purity of the as-prepared products. The diffraction peaks from both the ball- and star-shaped products can be indexed to rock

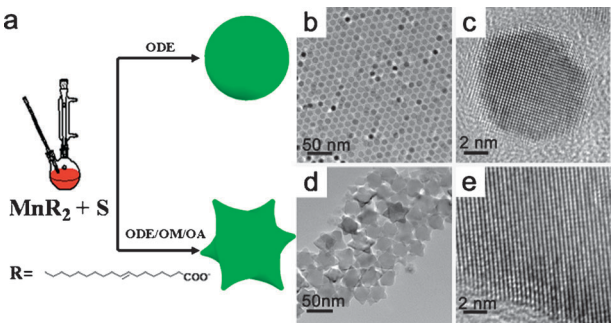

Fig. 1 (a) Schematic illustration of spherical and star-shaped α-MnS NCs prepared under different conditions, and corresponding TEM and HRTEM images of spherical (b, c) and star-shaped (d, e) NCs.

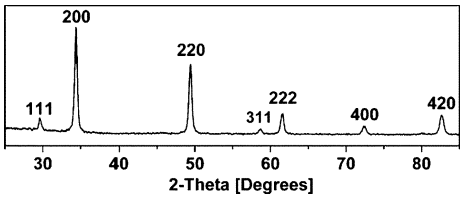

Fig. 2 XRD pattern of as-prepared star-shaped α-MnS NCs.

salt α-MnS with lattice constant of $a = 5.220$ Å, which agrees well with the reported value ($a = 5.221$ Å) (JCPDS card no. 65-2919). No characteristic peaks for impurities, such as elemental S or MnO, are observed.

Careful high-magnification TEM and electron diffraction (ED) examinations, Fig. 3a–c, clearly shed light on the structure of these well-defined star-shaped MnS NCs. In Fig. 3a, the NC displays a starfish symmetrical architecture, in which six branches appear to have slightly tipped ends and stretch out on a copper grid during the TEM imaging. The inset of Fig. 3a shows its corresponding ED pattern, in which the spots can be indexed as that along the [111] zone axis of crystalline α-MnS, indicating that this star-shaped NC is a single crystal with six branches growing along the ⟨100⟩ direction. In Fig. 3b and c, the NC appears as a asymmetrical tetragonal architecture, in which one/two of the branches is/are hidden beneath or protrudes vertically out of the structure, and thus overlapped due to tilting the sample in the TEM imaging, whereas its corresponding ED pattern is accordingly changed from [111] zone axis to [100] and [1$\bar{1}$0] zone axis, respectively. Fig. 3d–f give their corresponding 3D schematic models viewed from different observation directions, further suggesting that the MnS NCs exhibit a well-defined star-shaped architecture with six-fold symmetrical geometry. These results indicate that the MnS NCs are genuine starfish shaped architectures considering the two-dimensional projection of the three-dimensional six-branch stars standing on the substrate.

To further examine a cooperative effect of the mixed surfactants on the shape evolution of the MnS NCs, a series of experiments was performed. Without an addition of OA and OM in the ODE solution, thermal decomposition at 300 °C for 30 min, led to uniform spherical MnS NCs with a diameter of ~10 nm, Fig. 1b. If 1 mL of OA was added alone into the ODE solution, no NCs are observed even at a temperature as high as 320 °C for 1 h, suggesting that the MnS NCs can not form under acidic condition. If only OM is used as the surfactant, thermal decomposition occurs at 250 °C for 2 min, and irregular NCs with a diameter of 25 nm formed, Fig. S1 (ESI†), indicating that OM is an efficient activation reagent to accelerate forming NCs, as in previous reports.[22] However, by striking comparison, Fig. 1c shows that well-defined and uniform star-shaped MnS NCs are synthesized with a 1 : 1 mixture of OM and OA by volume in the ODE solution. Considering the results with OA or OM as sole surfactants, it suggests that the cooperative effect of OA and OM has a great influence on the formation of well-defined star-shaped NCs.[23] Also, the reaction temperature and time were examined in our synthetic process, it is found that when the temperature was lower than 260 °C, the star-shaped MnS NCs can not form, but rather irregular crystals, Fig. S2 (ESI†), and if the reaction time is longer than 15 min, the six branches of the star-shaped MnS NCs are blunt, *i.e.*, the above well-defined star-shaped morphology can not form, Fig. S3 (ESI†).

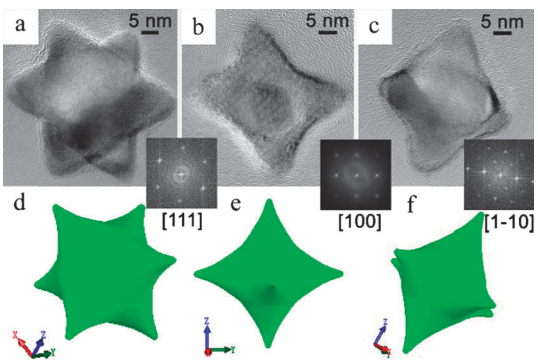

Fig. 3 (a), (b) and (c): High-magnification TEM images and their ED patterns (inset) of star-shaped MnS NCs with [111], [100] and [1$\bar{1}$0] zone axis, respectively. (d), (e) and (f): Schematic models show the corresponding NCs viewed from different observation directions, respectively.

Similar reaction systems, *i.e.*, fatty acid as a stabilization/coordination reagent and primary amine as an efficient activation reagent to accelerate the formation of nanoparticles, have been reported to prepare many kinds of well-defined shaped nanoparticles such as TiO_2,[22] $NaLa(MoO_4)_2$,[23] Fe_2O_3,[24] $MnFe_2O_4$[25] and ZnSe.[26] Since the crystal growth rate on different faces, which is closely related to the crystal surface energy, strongly governs the final shape of crystals, it is important to examine the surface energy related effects on the anisotropic growth of NCs.[27] It is well known that the intrinsic surface energy of the {111} faces of cubic α-MnS, containing Mn or S only, is lower than that of the {100} faces, containing a mixture of Mn and S.[27] However, in our reaction system, the carboxy groups of the deprotonated OA are typical electron donors and can thus strongly interact with electron-poor Mn atoms at the charged and low surface energy {111} faces rather than the uncharged and high surface energy {100} faces of α-MnS, restraining the growth of the {111} faces and accordingly promoting the preferential growth of the {100} faces. Hence, the activation of OM has a smaller effect on the growth rate of ⟨111⟩ direction, but greater effect on the growth rate of ⟨100⟩ direction of α-MnS. As a result, the difference of the relative growth rate between the surfaces with low activation barrier ({100} faces) and the surfaces with high activation barrier ({111} faces) is diminished by the deprotonated OA from the Mn oleate, and spherical MnS NCs were obtained through the thermal decomposition in hot ODE solution without the OM and OA. Considering that the activation of the OM makes the growth rate of {100} faces much higher than that of the {111} faces, irregularly star-shaped MnS NCs with six-branches along ⟨100⟩ directions formed through adding OM to ODE solution. When both OM and OA were added into the ODE solution, the activation of the OM will be reduced through forming an acid–base complex.[23] Therefore, a suitable ratio of OA to OM $<1:1$ (volume ratio) is still favorable for the formation of irregularly star-shaped α-MnS NCs, Fig. S4 (ESI†), and an optimal ratio of OA to OM, resulting in well-defined and uniform star-shaped α-MnS NCs, is ~1 : 1.

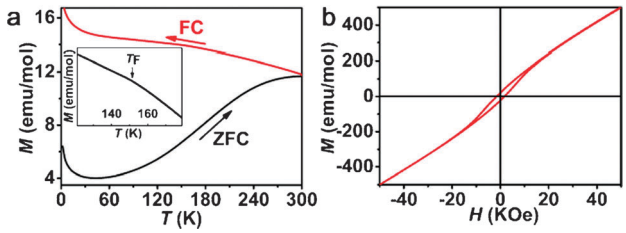

Fig. 4 (a) FC (red) and ZFC (black) curves, and inset showing a decrease of the magnetization at ~150 K. (b) Hysteresis loop of the star-shaped α-MnS NCs.

The successful synthesis of the well-defined star-shaped α-MnS NCs allows us to investigate their magnetic properties. Fig. 4a shows the temperature dependence of magnetization in the zero-field-cooled (ZFC) and field-cooled (FC) processes with an applied field of 500 Oe for the star-shaped MnS NCs. Similar to the nanosized γ-Fe_2O_3 particles,[28] it can be seen that the ZFC curve exhibits a typical blocking process with a high blocking temperature, T_B, at ~275 K. Importantly, the FC curve reveals an increase of magnetization below T_F ~ 150 K (Fig. 4a, inset), which is related with the onset of the freezing process of the surface spin-glass layer for the star-shaped MnS NCs. Considering that α-MnS NCs are antiferromagnetic, such a spin-glass-like behavior is denoted as a surface effect, since the Mn state at the surface is not the same as that inside a NC. This can be simply explained by a "core–shell type structure", which is similar to octahedral α-MnS NCs,[21] $Li_4Mn_5O_{12}$ nanosticks,[29] and CuO nanowires.[30] The main interactions occur between the spins of the core, which is antiferromagnetic, and the spins of the shell, which is insulating and disordering. The existence of a distorted structure at the surface of the MnS NCs is further supported by the hysteresis in Fig. 4b. The hysteresis of the star-shaped MnS NCs, measured at 2 K and 50 KOe, shows that the NCs are far from being magnetically saturated even at 50 KOe. More interestingly, the star-shaped MnS NCs show a large coercive field of 1573 Oe. This indicates that at low temperature the coercivity associated with some ferromagnetic materials is also present on the MnS NCs. Due to a large surface area of the star-shaped α-MnS NCs, this makes the shell comprise more uncompensated spins, inducing a high blocking temperature and a large coercive field, as compared with those of octahedral α-MnS NCs for which the blocking temperature is 23 K and the coercive field is 44 Oe, respectively.[21]

In summary, we have developed an effective method to control growth of well-defined star-shaped α-MnS nanocrystals *via* a cooperative thermal decomposition route using the mixed surfactant of OM and OA; these star-shaped α-MnS nanocrystals show novel magnetic properties, *i.e.*, a high blocking temperature (275 K) and a large coercive field (1573 Oe), as compared with the previous reports on α-MnS nanocrystals, which is due to the main interactions between the spins of the core (antiferromagnetic) and the spins of the shell (insulating and disordering). The present studies of the star-shaped α-MnS nanocrystals not only extend the understanding of crystal growth but are also technologically promising in terms of the novel magnetic properties of this material.

This work was financially supported by the Program for New Century Excellent Talents of the University in China (Grant No. NCET-08-0761), the National Natural Science Foundation of China (Grant No. 50872020 and 50902021), the "Pujiang" Program of Shanghai Education Commission in China (Grant No. 09PJ1400500), the "Dawn" Program of Shanghai Education Commission in China (Grant No. 08SG32), the Science and Technology Commission of Shanghai-based "Innovation Action Plan" Project (Grant No. 10JC1400100), Specialized Research Fund for the Doctoral Program of Higher Education (Grant No. 20090075120014), "Chen Guang" project (Grant No. 09CG27) supported by Shanghai Municipal Education Commission and Shanghai Education Development Foundation, the Fundamental Research Funds for the Central Universities, and the Innovation Foundation of DHU for PhD Graduates (No. BC20101225).

Notes and references

1 J. T. Hu, T. W. Odom and C. M. Lieber, *Acc. Chem. Res.*, 1999, **32**, 435.
2 G. Markovich, C. P. Collier, S. E. Henrichs, F. Remacle, R. D. Levine and J. R. Heath, *Acc. Chem. Res.*, 1999, **32**, 415.
3 S. M. Lee, Y. W. Jun, S. N. Cho and J. Cheon, *J. Am. Chem. Soc.*, 2002, **124**, 11244.
4 B. H. Wu, N. F. Zheng and G. Fu, *Chem. Commun.*, 2011, **47**, 1039.
5 N. Zhao and L. M. Qi, *Adv. Mater.*, 2006, **18**, 359.
6 J. Zeng, Y. Q. Zheng, M. Rycenga, J. Tao, Z. Y. Li, Q. A. Zhang, Y. M. Zhu and Y. N. Xia, *J. Am. Chem. Soc.*, 2010, **132**, 8552.
7 Y. G. Sun and Y. N. Xia, *Science*, 2002, **298**, 2176.
8 N. Tian, Z. Y. Zhou, S. G. Sun, Y. Ding and Z. L. Wang, *Science*, 2007, **316**, 732.
9 N. Pradhan, H. F. Xu and X. G. Peng, *Nano Lett.*, 2006, **6**, 720.
10 Z. A. Peng and X. G. Peng, *J. Am. Chem. Soc.*, 2002, **124**, 3343.
11 J. K. Furdyna and N. Samarth, *J. Appl. Phys.*, 1987, **61**, 3526.
12 D. S. Kim, J. Y. Lee, C. W. Na, S. W. Yoon, S. Y. Kim, J. Park, Y. Jo and M. H. Jung, *J. Phys. Chem. B*, 2006, **110**, 18262.
13 N. Zhang, R. Yi, Z. Wang, R. R. Shi, H. D. Wang, G. Z. Qiu and X. H. Liu, *Mater. Chem. Phys.*, 2008, **111**, 13.
14 Y. Cheng, Y. S. Wang, C. Jia and F. Bao, *J. Phys. Chem. B*, 2006, **110**, 24399.
15 Y. H. Zheng, Y. Cheng, Y. S. Wang, L. H. Zhou, F. Bao and C. Jia, *J. Phys. Chem. B*, 2006, **110**, 8284.
16 S. Biswas, S. Kar and S. Chaudhuri, *J. Cryst. Growth*, 2007, **299**, 94.
17 S. Biswas, S. T. Kar and S. Chaudhuri, *Mater. Sci. Eng., B*, 2007, **142**, 69.
18 L. Tian, L. Y. Yep, T. T. Ong, J. B. Yi, J. Ding and J. J. Vittal, *Cryst. Growth Des.*, 2009, **9**, 352.
19 Y. W. Jun, Y. Y. Jung and J. Cheon, *J. Am. Chem. Soc.*, 2002, **124**, 615.
20 J. Joo, H. B. Na, T. Yu, J. H. Yu, Y. W. Kim, F. X. Wu, J. Z. Zhang and T. Hyeon, *J. Am. Chem. Soc.*, 2003, **125**, 11100.
21 A. Puglisi, S. Mondini, S. Cenedese, A. M. Ferretti, N. Santo and A. Ponti, *Chem. Mater.*, 2010, **22**, 2804.
22 Z. H. Zhang, X. H. Zhong, S. H. Liu, D. F. Li and M. Y. Han, *Angew. Chem., Int. Ed.*, 2005, **44**, 3466.
23 W. B. Bu, Z. X. Chen, F. Chen and J. L. Shi, *J. Phys. Chem. C*, 2009, **113**, 12176.
24 T. Hyeon, S. S. Lee, J. Park, Y. Chung and H. Bin Na, *J. Am. Chem. Soc.*, 2001, **123**, 12798.
25 H. Zeng, P. M. Rice, S. X. Wang and S. H. Sun, *J. Am. Chem. Soc.*, 2004, **126**, 11458.
26 S. L. Lin, N. Pradhan, Y. J. Wang and X. G. Peng, *Nano Lett.*, 2004, **4**, 2261.
27 Y. W. Jun, J. H. Lee, J. S. Choi and J. Cheon, *J. Phys. Chem. B*, 2005, **109**, 14795.
28 B. Martinez, X. Obradors, L. Balcells, A. Rouanet and C. Monty, *Phys. Rev. Lett.*, 1998, **80**, 181.
29 M. H. Xu, W. Zhong, J. Y. Yu, W. C. Zang, C. Au, Z. X. Yang, L. Y. Lv and Y. W. Du, *J. Phys. Chem. C*, 2010, **114**, 16143.
30 C. Diaz-Guerra, M. Vila and J. Piqueras, *Appl. Phys. Lett.*, 2010, **96**, 193105.

